Paper Ref No: ICF100764OR

FATIGUE CRACK GROWTH PREDICTIONS IN AA 5083 AND AA 2024 USING A SIMPLE GEOMETRIC MODEL.

Ton Riemslag(1), Kees van Kranenburg(1), Saskia Benedictus-de Vries(1), Fred Veer(2) and Jan Zuidema(1)(*)

(1) Laboratory of Materials Science, Delft University of Technology
(2) Faculty of Architecture, Delft University of Technology
E-mail to: j.zuidema@tnw.tudelft.nl

Abstract

Constant amplitude fatigue crack growth tests conform ASTM E647 are performed on AA 5083-H321 for different R-values in air and seawater. Fatigue crack growth starts in the flat tensile mode, but after some crack advance shear lips start on both sides of the fracture surface. The shear lips grow in width on further crack growth until (almost) the total crack surface has become slanted. The start and growing in width of the shear lips is accompanied by a decrease in crack growth rate, resulting in a change to a lower slope of da/dN-ΔK on double-logarithmic scale. When the shear lips cover the total fracture surface the original slope of da/dN versus ΔK is almost restored. Crack closure relations for several parts of da/dN versus ΔK have been found. A simple macroscopic geometrical model is made in order to predict fatigue crack growth behaviour in the shear lip crack growing area. The model is also applied to a situation with underloads in AA 2024-T351.

Keywords

crack closure, shear lips, underloads, crack growth prediction

Introduction

The fatigue crack growth properties of two aluminum alloys, AA 2024 and AA 5083, are compared. The AlCuMg Aluminium Alloy AA 2024 is widely used in both civil and military aircraft because of its superior damage tolerance and fatigue properties. The AlMgMn Aluminium Alloy AA 5083 is increasingly used in shipbuilding, including high-speed ferries, because of its good mechanical properties and excellent corrosion (fatigue) resistance. Both materials have been fatigued in laboratory air and AA 5083 also in seawater. The difference in fatigue fracture behaviour is described in terms of differences in macroscopic fracture surface and different corrosion-fatigue behaviour. Crack closure was accounted for by varying the stress ratio. Especially transitions in the crack growth rate, that are accompanied by developing shear lips, form a subject of study. The shear lips grow in width as the crack length increases, but there exists no direct correlation between start of shear lips and transition in crack growth rate. It will be shown that suppression of shear lip initiation and growth also shows the same transitions.

For both materials the shear lip starts at about the same crack growth rate da/dN, at which value also the slope change in da/dN-ΔK occurs, but both events are dependent on the environment. When the shear lips cover the total fracture surface the original slope of da/dN versus ΔK is changed again. Crack closure relations for AA 5083 for some parts of da/dN versus ΔK have been found. A simple macroscopic geometrical model is made in order to

predict fatigue crack growth behaviour in the shear lip crack growing area, using crack growth rate data from the area without shear lips.. The principle of the calculation is that the K factor and the shear lip width are both influenced by the same, yet unknown (micro)mechanism. The shear lip width is then considered as a measure for K. The developing shear lip width rate is assumed to be proportional to the difference in actual shear lip width and the equilibrium shear lip width, being the width as would be found in a constant ΔK test after a large enough crack growth.
Furthermore the model is applied to a situation with underloads in AA 2024. The underloads are high enough to give rise to slanted crack growth. The crack growth behaviour after different numbers of underloads is both measured and predicted.

Experiments

The chemical composition of the materials is as shown in the table:

TABLE CHEMICAL COMPOSITION(WT %) OF AA 5083 AND 2024, REMAINDER AL

AA	Mg	Mn	Si	Fe	Cr	Cu	Zn	Ti
5083	4.5	0.65	0.26	0.22	0.09	0.09	0.06	0.03
2024	1.18	0.67	0.34	0.14	0.004	4.75	0.19	0.03

The center-cracked specimens have a length of 340 mm, a width of 100 mm and a thickness of 8 mm (AA 5083) or 6 mm (AA 2024). The fatigue crack growth experiments are performed on a computer-controlled servohydraulic fatigue machine. The loading program is

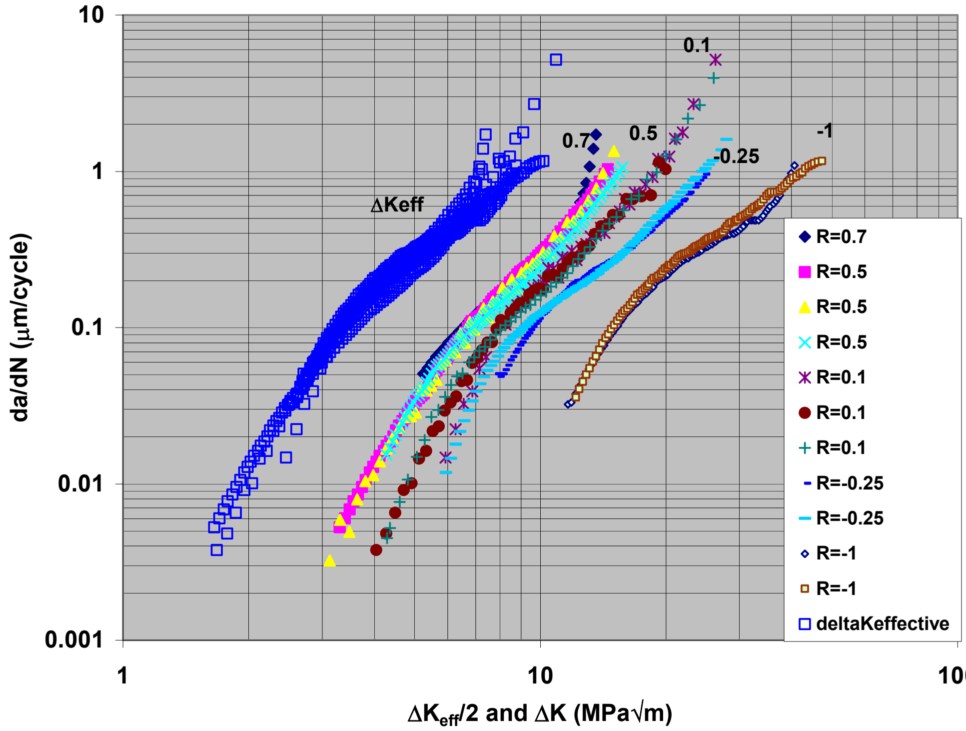

Figure 1. Results of 11 constant amplitude tests on AA 5083 at 5 different values of R and the corresponding da/dN-ΔK_{eff} (shifted a factor 2 to the left for clearness).

offered to the machine in the form of a load table where the maximum load, the minimum load, the crack length and the frequency are specified.. The crack length is measured using a pulsed direct-current potential drop measurement system. The frequency is 10 Hz.

Results

The results from 11 constant load amplitude tests on material AA 5083 in air are shown in figure 1. It can be noticed that at about da/dN = 0.1 μm/cycle, the crack growth rate curves change in slope. Observations of the different fracture surfaces revealed that at the corresponding ΔK-values the crack appearance started changing from flat to slant. At first the change in slope was attributed to a possible different crack closure situation due to the growing shear lips. But it was shown that suppression of shear lips leads to the same change of slope, thus extra closure due to shear lips probably doesn't exist in AA 5083. As the start of shear lips corresponds with different K_{max}-values (e.g. K_{max} = 8.8 and 13 MPaŒm respectively for R = 0.1 and 0.5), it can be concluded that the start of the shear lips is also probably not a matter of plane stress/plane strain. The only obvious correlation is with the crack growth rate or, which is equivalent, with the ΔK_{eff}. This is in agreement with observations on AA 2024 [1]. In seawater the change in slope starts at about 0.2 μm/cycle, at 10 Hz [2].

Crack closure relations

For AA 2024 the well-known relation of Elber will be used, with U=0.5+0.4R for $-0.1 < R < 0.7$. This relation fits the results for AA 5083 not very well. Crack closure for this alloy is not measured directly, but it is found by correlating 7 of the 11 constant amplitude da/dN versus ΔK results shown in figure 1. One test at R=0.7, one test at R=0.5, two tests at R=0.1, one test at R=-0.25 and two tests at R=-1. The best quadratic crack closure function $U= a+bR+cR^2$ is found by taking all combinations of a, b and c and calculating $\Delta K_{eff}=U\Delta K$ for all measurement points of the 7 tests. A power formula of type $da/dN=C\ \Delta K_{eff}{}^m$ is fitted through the da/dN-ΔK_{eff} points. The combination of a, b and c with a maximum value of the correlation coefficient, based on log(da/dN) and log(ΔK_{eff}), is considered the best combination. The combination is normalized, i.e. the normalized coefficients are found by dividing the best calculated coefficients by their sum, meaning that U=1 if R=1. The best crack closure formula found in this way for this material is $U=0.66+0.32R+ 0.02R^2$. The formula for the best power fit is given in equation 1, where da/dN in (μm/cycle) and ΔK_{eff} in (MPaŒm):

$$da/dN=0.70*10^{-3}\ \Delta K_{eff}{}^{2.8} \qquad (1)$$

However the results in figure 1 show that the curves for R=0.5 and 0.7 are about the same, meaning that crack closure is not important above R=0.5. If it is assumed that U=1 already for R>=0.5, then this constraint can be added to the calculation procedure. The result of the calculation is now $U=0.80+0.39R+ 0.03R^2$ for R<=0.5 and U=1 for R>0.5. With this constraint da/dN can be calculated as:

$$da/dN=0.41*10^{-3}\ \Delta K_{eff}{}^{2.8} \qquad (2)$$

The same crack closure calculation was also applied using only datapoints without shear lips, i.e. for da/dN<0.1 μm/cycle. For the constraint situation with U=1 for R=1, the result is $U=0.65+0.32R+0.03R^2$ and

$$da/dN=0.80*10^{-4}\ \Delta K_{eff}{}^{4.16} \qquad (3)$$

The da/dN-ΔK_{eff} fit result for the constraint situation with U=1 for R=1, eq.1, is also shown in figure 1 for all data points at different R. A parallel shift is applied to better show the result, i.e. the corresponding ΔK_{eff} results have to be multiplied by a factor of 2.

The geometric crack growth prediction model

Although the start of shear lips is not the cause of the change in slope of the log(da/dN)-log(ΔK) line, it seems to be a consequence of another, not yet known (micro)mechanism, that results in both shear lip start and growth and also in a lower slope of the log(da/dN)-log(ΔK) relation. The shear lip width is chosen to represent this unknown mechanism. It was shown in reference 1 that shear lips grow in width, even in a constant ΔK test, until an equilibrium width has been reached. A linear relation was found between equilibrium width and ΔK_{eff} for AA 2024. An equivalent behaviour for AA 5083 was assumed. In figure 2 a fatigue fracture surface is shown. The shear lip is suppressed on one side of the specimen by making a scratch with a depth of 0.1 mm along the crack growth direction.

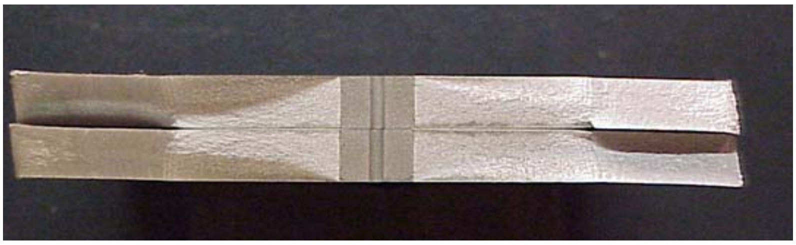

Figure 2. Shear lips suppressed on one side in AA 5083.

Hardly any difference was found in crack growth rate between specimens with scratches on both sides, where shear lips were fully suppressed, or specimens with shear lips on one side or specimens with full shear lips. Also the change in slope occurred equally, for da/dN=0.1 μm/cycle, in all three different kind of specimens. Based on a preliminarily study of the fracture surfaces the equilibrium shear lip width is estimated (for $t_{s,eq} > 0$):

$$t_{s,eq} = 0.90\Delta K_{eff} - 5 \text{ (mm)} \tag{4}$$

If the actual $t_{s,eq}$ and ΔK_{eff} do not fulfill this equation, the shear lip width will increase or decrease until the equilibrium situation is reached, according to the equation given above. The rate of change in shear lip width is taken proportional with the difference in actual width and equilibrium width, in formula form:

$$dt_s/da = C(t_{s,eq} - t_s) \tag{5}$$

For AA 5083 the C-value is estimated as:

$$C = 0.40/t_{s,eq} \quad (\text{mm}^{-1}) \tag{6}$$

In a constant amplitude test the ΔK_{eff} changes continuously and hence also $t_{s,eq}$ and t_s; t_s lags behind $t_{s,eq}$ for the growing crack. It is assumed that the crack driving force ΔK is influenced by the slope changing (micro)mechanism and that the shear lip width is a measure for it. The ΔK that is responsible for the lower da/dN increase in the shear lip area and beyond is called ΔK(shear). It is defined as:

$$\Delta K(\text{shear}) = \Delta K/(1+2(\sqrt{2}-1)t_s/t) \tag{7}$$

It means that the product of ΔK and the transverse crack length is assumed to be constant. If a shear lip angle of 45° is taken $\Delta K(\text{shear}) = \Delta K/\sqrt{2}$ for a complete slanted surface with $t_s = t/2$, and for $t_s = 0$ it gives $\Delta K(\text{shear}) = \Delta K$.

A computer program was written to calculate ΔK(shear) as a function of the crack length for constant amplitude tests. Also da/dN versus ΔK is calculated, using the da/dN-ΔK equation in the crack growth area without shear lips.

Result of the prediction

The prediction is tested on the crack growth rate result for R=0.1 as shown in figure 3. The slope of the results is about 5.5 for da/dN<0.1 μm/cycle, above which value it transforms to about 2.5 until da/dN =1 μm/cycle. From 1 to 10 μm/cycle the slope is again about 5. Above 10 μm/cycle static effects are probably superposed on the fatigue crack growth rate. For the calculation of ΔK the ASTM formula for a centre-cracked tension specimen (width w) is used:

$$K = \sigma\sqrt{\pi a}\sqrt{\sec\frac{\pi a}{w}} \tag{8}$$

The prediction is quite well in the shear lip developing area. Static effects have not been incorporated in the calculation.

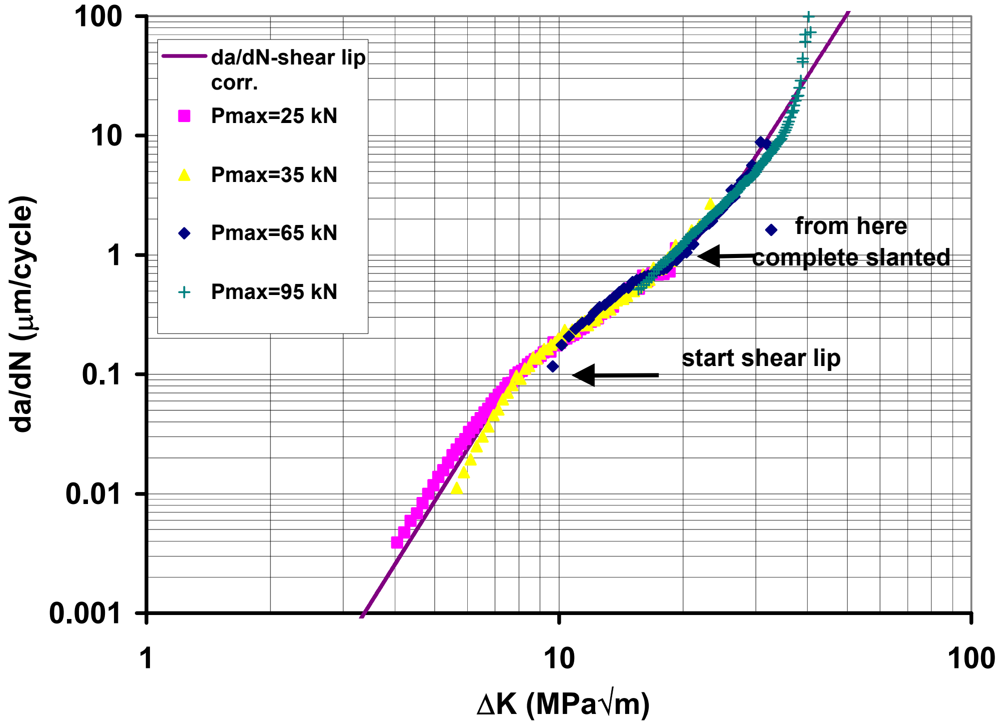

Figure 3 Experimental fatigue crack growth rate results and prediction for AA5083 at R=0.1

Underloads in AA 2024

Constant ΔK tests with constant ΔK underloads were performed in AA 2024. The underloads were high enough to lead to development of shear lips, while the ΔK before and after the underloads were to low for it. All K_{max} were the same to avoid plasticity induced crack closure at the loading transitions. A retardation in crack growth rate was measured after the underloads. The retardation was larger for higher ΔK of the underloads and for more underload cycles. The shear lips vanished quickly after the underloads, but the retardation of the crack growth rate lasted about three times as long, i.e. if there is an effect of the shear lips on ΔK, it extends outside the area where shear lips are really present. The same calculation is applied as on AA 5083, only now, in this situation of decreasing and vanishing shear lip width, ΔK is not assumed to be influenced by the real shear lip width at the crack tip, but by a mean of the shear lip width extending over some mm crack length after the tip. Calculations taking the actual shear lip width at the tip as a measure for ΔK, and calculations taking the mean shear lip width over 3 mm after the tip were applied and compared with a real test with underloads, see figure 4. The 3 mm was estimated using a potential drop measurement of the affected crack length by crack closure in this case.

A possible explanation of the change in slope.

The following explanation is rather speculative at the moment. It is found that in AA 5083 the change in slope starts at 0.1 μm/cycle in air and at 0.2 μm/cycle in seawater [2]. The change in slope is independent of K_{max} or ΔK. Earlier investigation on AA 2024 in vacuum did result in a change of slope at about 0.004 μm/cycle (for R=0.3). These results indicate that the reason of the change in slope is not due to mechanically causes alone, but that it more depends on the environment. Suppose that a corrosion reaction is responsible for enhanced fatigue crack growth below the transition, i.e. below 0.1 µm/cycle in air.

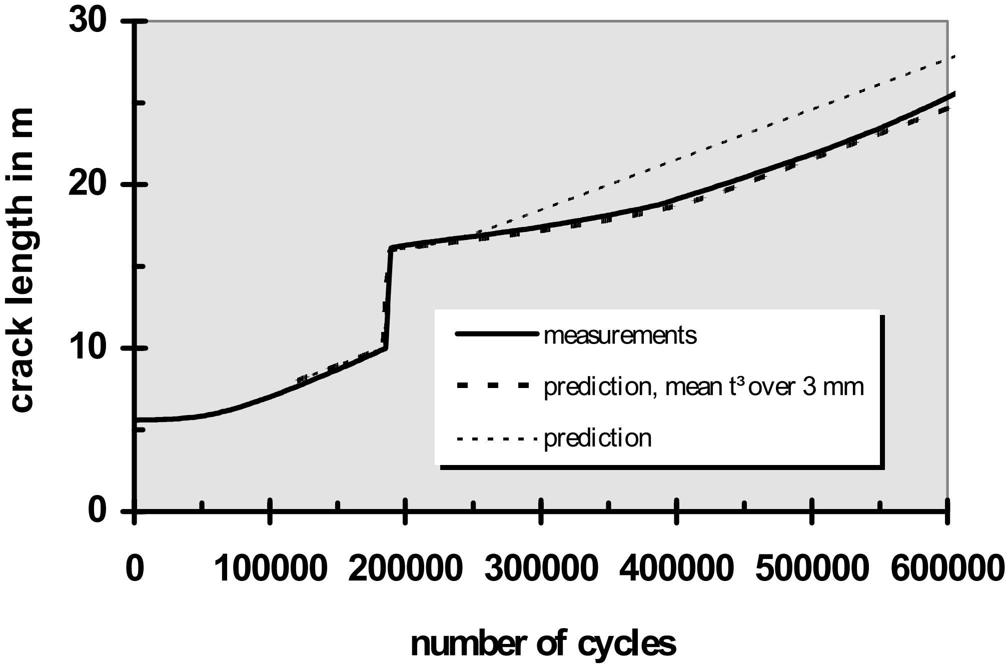

Figure 4. Measurements and prediction of the a-N curve in AA 2024 with 5000 underloads, underload sequence ΔK=5-16-5 (MPaŒm) at K_{max} = 29 (MPaŒm) and 10 Hz.

Above this crack growth rate the crack moves too fast for the corrosion assisted mechanism to take fully place, and the intrinsic fatigue crack growth rate will increasingly dominate, with a growing slanted crack surface as a result. Seawater is a more aggressive environment, and it can be expected that a higher crack growth rate than in air is needed to outrun the corrosion reaction speed. In vacuum the reverse is true and the transition will take place at a very low value of the crack growth rate. We will at the moment not speculate on the exact mechanism of the corrosion reaction, but following this rationale it is clear that the fatigue fracture situation with shear lips is the “normal” fatigue crack growth mode in these Al Alloys. When the fracture surface is flat, it is so by an environmental attack.

Conclusions

1) The shear lip width seems to be a good measure for the transition from fast crack growth rate due to environmental attack to slower intrinsic true fatigue crack growth rate after the transition point.
2) The enhanced crack growth rate at lower da/dN is due to environmental attack.

References

1) Zuidema, J. and M. Mannesse, *A model for predicting slant crack growth in Al 2024*. Engineering Fracture Mechanics 34 ,1989, 2, p.445-456’
2) Jan Zuidema, Saskia de Vries and Adirakhmantyo Hascaryantono,*The Accelerated ΔK Fatigue Crack Growth Test on AA 5083-H321 and Similitude Validation,*The 13th European Conference on Fracture ECF 13, 6th-9th september, 2000, San Sebastian, Spain.